

## Dipped adcluster model study for the end-on chemisorption of O<sub>2</sub> on an Ag surface

HIROSHI NAKATSUJI<sup>1</sup> AND HIROMI NAKAI

*Department of Synthetic Chemistry, Faculty of Engineering, Kyoto University, Kyoto 606, Japan*

Received June 10, 1991

*This paper is dedicated to Professor Sigeru Huzinaga on the occasion of his 65th birthday*

HIROSHI NAKATSUJI and HIROMI NAKAI. *Can. J. Chem.* **70**, 404 (1992).

Theoretical study for the end-on adsorption of an O<sub>2</sub> molecule on an Ag surface is carried out with the use of the dipped adcluster model (DAM). The adcluster of AgO<sub>2</sub> is taken and the highest spin coupling model is employed. Electron transfer from the bulk metal to the adcluster considered by DAM is important for the occurrence of the chemisorption, and this cannot be described by the small-size cluster model. Electron correlations are also quite important and are described by the SD-CI method based on the corresponding parent configurations. In the end-on geometry, the superoxide species is the ground state, and there are no peroxide species in the lower energy region. The calculated adsorption energy compares reasonably with the experimental value. The O—O axis of the superoxide is inclined by 70°–80° from the surface normal. The outside oxygen atom of the adsorbed species seems to be more reactive than the inside one, while the net charge on the former is smaller than that on the latter.

**Key words:** DAM (dipped adcluster model), silver, superoxide, chemisorption.

HIROSHI NAKATSUJI et HIROMI NAKAI. *Can. J. Chem.* **70**, 404 (1992).

Utilisant le modèle de l'«adagrégat» plongé (DAM), on a effectué une étude théorique de l'adsorption par le bout de la molécule d'oxygène sur une surface. On a pris l'«adagrégat» du AgO<sub>2</sub> et on a utilisé le modèle du couplage des spins les plus élevés. Sur la base du DAM, le transfert d'électron de l'ensemble du métal vers l'«adagrégat» semble une condition importante pour que la chemisorption puisse se produire; cette importance ne peut pas être décrite par le modèle des petits agrégats. Les corrélations d'électrons sont aussi très importantes et elles peuvent être décrites par la méthode SD-CI basée sur les configurations des parents correspondants. Dans la géométrie d'addition par le bout, l'espèce superoxyde est dans l'état fondamental et il n'y a pas d'espèce peroxyde dans la région d'énergies plus faibles. L'énergie d'adsorption calculée se compare raisonnablement bien avec la valeur expérimentale. L'axe O—O du superoxyde est incliné de 70° à 80° par rapport à la surface normale. L'atome d'oxygène qui se trouve à l'extérieur de l'espèce adsorbée semble plus réactif que celui qui se trouve à l'intérieur alors que la charge nette du premier est plus faible que celle du dernier.

**Mots clés :** DAM (modèle de l'«adagrégat» plongé), argent, superoxyde, chemisorption.

[Traduit par la rédaction]

### Introduction

An oxygen molecule adsorbed on a silver surface can undergo several important catalytic reactions. In particular, the partial oxidation of ethylene (1) is a very useful reaction in chemical industry. Several studies for clarifying the nature of the adsorbed oxygen have been performed in order to understand the mechanism of this reaction (2–4). However, there still remain many questions about the structure and electronic states of the adsorbed oxygen species involved in the epoxidation.

Two different observations have been made about the structure of the adsorbed oxygen. The NEXAFS study of O<sub>2</sub>/Ag(110) shows that the O—O axis is parallel to the surface along the [1 $\bar{1}$ 0] azimuthal axis with the O—O distance of  $1.47 \pm 0.05$  Å (5). The ESDIAD experiment of O<sub>2</sub>/Ag(110) indicates that O<sub>2</sub> is bonded end-on to a single Ag atom, slightly inclined away from the surface normal along the [001] azimuth (6).

In our previous study (7), we examined a side-on adsorption of O<sub>2</sub> onto an Ag surface by using the dipped adcluster model (DAM) (8, 9) combined with the SAC (symmetry adapted cluster)/SAC-CI method (10, 11). It has been shown that two superoxide (O<sub>2</sub><sup>-</sup>) and one peroxide (O<sub>2</sub><sup>2-</sup>) species exist in that geometry, while the latter is 13 kcal/mol more stable than the former. The peroxide species leads to dissociative adsorption with further stabilization. It was con-

cluded that electron correlations in low-lying surface states and electron transfer from bulk metal to the adcluster are important for the oxygen chemisorption. The heats of molecular and dissociative chemisorptions and the O—O vibrational frequencies agreed well with the experimental values. In addition to other theoretical studies (12–16) on the side-on adsorptions of O<sub>2</sub> onto the silver surface, which use the cluster model, the structures and electronic states of the side-on oxygen species are considerably clarified.

In this study, we investigate the end-on adsorption of an O<sub>2</sub> molecule on an Ag surface with the use of DAM. Electron correlation is described by the SD-CI method based on the respective parent configurations. On the other hand, cluster-model SCF calculations for AgO<sub>2</sub> were carried out by Broomfield and Lambert (17). They showed the existence of two superoxide species in the end-on geometry with inclined O—O axis, but no stabilization energies were presented.

### Dipped adcluster model

The dipped adcluster model was proposed as a theoretical model for studying chemisorptions and surface reactions involving electron transfers between ad molecules and surfaces (8, 9). The "adcluster," a combined system of an ad molecule and a cluster, is dipped onto the electron "bath" of a solid metal and an equilibrium is established for electron and (or) spin transfers between them. The equilibrium condition is described by using the chemical potentials of the

<sup>1</sup>Author to whom correspondence may be addressed.

adcluster and the solid surface. Namely, at equilibrium, the adcluster is at the  $\min[E(n)]$  in the range,

$$[1] \quad -\frac{\partial E(n)}{\partial n} \geq \mu$$

where  $E(n)$  is the energy of the adcluster, with  $n$  being the number of electrons transferred from the bulk metal to the adcluster and  $\mu$  the chemical potential of the electrons of the metal surface. While all the electrons transferred into the admolecule must be supplied by the cluster alone in the conventional cluster model, some of the electrons are supplied from the electron bath of the bulk metal in DAM. The admolecule charged by this electron transfer induces an electrostatic polarization on the metal surface and receives an electrostatic attractive force. In DAM, the energy of the adcluster is given by

$$[2] \quad E = E^{(0)} + E^{(1)}$$

where  $E^{(0)}$  is the electronic energy of the adcluster alone and  $E^{(1)}$  the energy of the electrostatic interaction between the adcluster and the bulk metal. For  $E^{(0)}$ , the molecular orbital model of the dipped adcluster was proposed (8) and, for  $E^{(1)}$ , estimation by the method of image force was suggested (9). The energy  $E$  of the system is calculated as a function of  $n$ .

In the present study, a linear  $\text{Ag}-\text{O}_a-\text{O}_b$  system is taken as an adcluster. At infinite separation, the  $\text{O}_2$  molecule is in the  ${}^3\Sigma_g^-$  state and the Ag atom in the  ${}^2S$  ( $d^{10}s^1$ ) state. The highest (or parallel) spin coupling model is adopted, since it gives a continuous picture leading to the correct separation limit. In the linear  $\text{AgO}_2$  system, the frontier MOs are mainly composed of the degenerate  $\pi^*$  MOs of  $\text{O}_2$ . Since the  $\pi^*$  orbitals of  $\text{O}_2$  are already singly occupied by two  $\alpha$ -spin electrons, an  $n/2$   $\beta$ -spin electron is added to each of the degenerate  $\pi^*$  orbitals.

The DAM calculations have been performed with the *ab initio* RHF SCF MO program. The Gaussian basis set for the silver atom is  $(3s3p4d)/[3s2p2d]$  and the Kr core is replaced by the relativistic effective core potential (18). For oxygen, we use the  $(9s5p)/[4s2p]$  set of Huzinaga-Dunning (19) augmented by the diffuse  $s,p$  functions of  $\alpha = 0.059$  as anion bases (20) and the polarization  $d$  function of  $\alpha = 0.30$ .

Figure 1 is a display of the  $E(n)$  curves, energy as a function of  $n$ . This figure is for the  $\text{Ag}-\text{O}_a$  distance at 2.20 Å, which is almost the most stable distance. The O—O distance is changed from 1.20741 Å, which is an equilibrium length of  $\text{O}_2$  (21), to 1.35 Å, which is an equilibrium length for  $\text{O}_2^-$  (22). The curves are upper convex and the curvature is discontinuous at  $n = 0.0$  and  $n = 1.0$ . At  $n = 0.0$ ,  $R_{\text{O}-\text{O}} = 1.20741$  Å is more stable, but at  $n = 1.0$ ,  $R_{\text{O}-\text{O}} = 1.35$  Å is more stable. The tangents of the curves coincide with the experimental chemical potential  $-\mu$  of the solid silver metal (4.52 eV) (23) at  $n = 0.7$ . Therefore, as judged from the equilibrium condition of eq. [1], one electron flows from the bulk metal into the adcluster after a certain barrier.

### $\text{O}_2$ approaching process

We next investigate the end-on approach of the  $\text{O}_2$  molecule to the silver surface. Electron correlations in the low-lying states of the adcluster are calculated by including all the single and double (SD) excitation configurations relative to the corresponding parent configurations. Zero- and

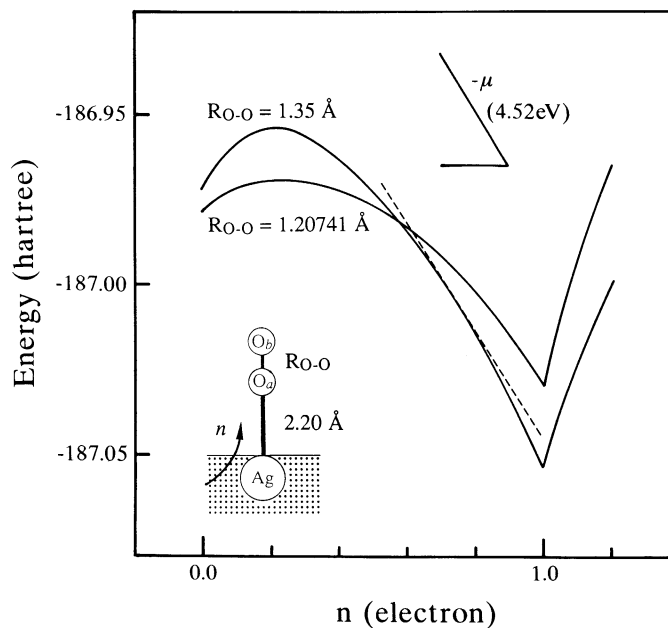


FIG. 1.  $E(n)$  curve for the  $\text{Ag}-\text{O}_a-\text{O}_b$  system in the highest spin coupling model with the  $\text{O}_a-\text{O}_b$  distance of 1.20741 and 1.35 Å, and the  $\text{Ag}-\text{O}_a$  distance of 2.20 Å.

one-electron transferred states are calculated in relation to the results of Fig. 1. The active space in the SD-CI calculations consists of 11 higher occupied orbitals and 16 lower unoccupied orbitals calculated by the HF method. The 11 occupied orbitals are mainly made up from the 4d and 5s atomic orbitals of Ag and the 2p atomic orbitals of O. The CI calculations are carried out with the use of the program GAMESS (24).

Figure 2 shows the potential energy curves for the approaching process. The ground state of the separated system, Ag plus  $\text{O}_2$ , corresponds to the  ${}^4\Sigma^+$  state. The energy of the separated system is estimated to be  $-187.089988$  hartree by SD-CI calculation of the supermolecule. On the other hand, it is estimated to be  $-187.108991$  hartree by SD-CI calculation of the free Ag plus  $\text{O}_2$  system, of which the active spaces are  $[6 \times 7]$  and  $[5 \times 9]$ , respectively. The energy scale on the right-hand side in Fig. 2 is in kcal/mol relative to the free system. The energy difference between the two estimations is due to the truncated nature of the CI method, which causes an unsatisfactory size consistency, as is well known. Therefore, the adsorption energy calculated from the CI of the separated free system is always smaller than that obtained from the CI for the supermolecule.

The  ${}^4\Sigma^+$  state does not involve electron transfer between the bulk metal and the adcluster. The potential energy curve of the  ${}^4\Sigma^+$  state rises monotonously as  $\text{O}_2$  approaches and shows that  $\text{O}_2$  is not adsorbed on the silver surface along this state. While the curve of the  ${}^4\Sigma^+$  state is calculated for  $R_{\text{O}-\text{O}}$  fixed at 1.20741 Å, a similar repulsive curve is also obtained for  $R_{\text{O}-\text{O}}$  fixed at 1.35 Å and lies at higher energy than the curve shown in Fig. 2.

On the other hand, the ground state of the adsorbed system is the  ${}^3\Pi$  state and involves one-electron transfer from the bulk metal. The potential energy curve of the  ${}^3\Pi$  state is attractive and has a minimum at the  $\text{Ag}-\text{O}$  distance of

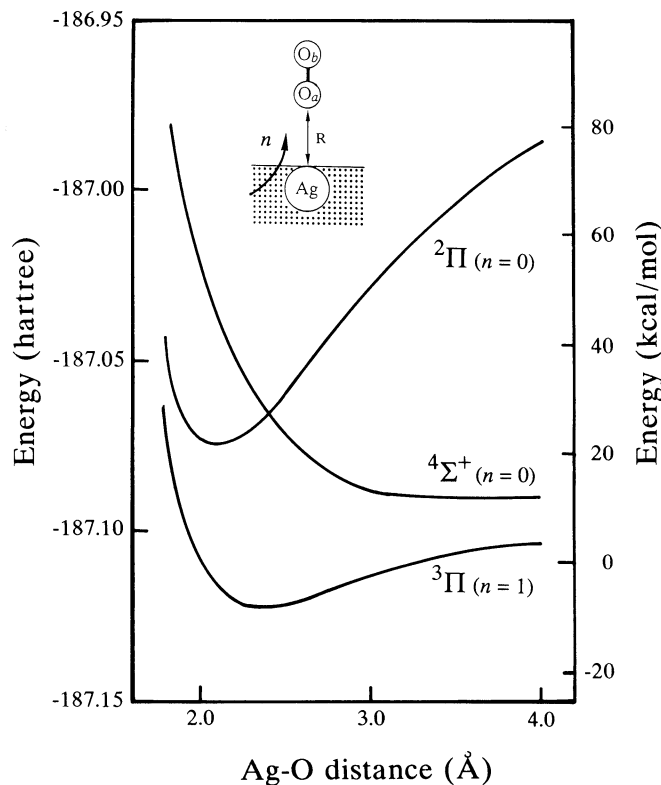


FIG. 2. Potential energy curves for the end-on approach of the  $O_2$  molecule onto silver, calculated by the SD-CI method. The O—O length is fixed at 1.20741 Å for the  $^4\Sigma^+$  state and at 1.35 Å for the  $^2\Pi$  and  $^3\Pi$  states.  $n$  denotes the number of electrons transferred into the adcluster from the bulk metal. The energy scale on the right-hand side is in kcal/mol relative to the free Ag plus  $O_2$  system.

2.2 Å. The  $^3\Pi$  state corresponds to the superoxide species  $O_2^-$ , since the degenerate  $\pi^*$  orbitals of  $O_2$  are formally occupied by three electrons. The adsorption energy of the superoxide is calculated to be 19.4 kcal/mol relative to the energy of the supermolecule, and to be 7.5 kcal/mol relative to the energy of the free system. These calculated adsorption energies are positive in both cases and comparable with the experimental value of 9.2 kcal/mol (25).

The  $^2\Pi$  state is an electron-transferred state from Ag to  $O_2$ , but no electron is supplied from the bulk metal. The potential energy curve of the  $^2\Pi$  state has a minimum at the Ag—O distance of 2.0 Å, but the energy is always higher than that of the separated system (negative adsorption energy). This state corresponds to the superoxide species obtained by the conventional cluster model, though the present potential energy contains the electrostatic energy correction  $E^{(1)}$ . This result shows that the electron transfer from the bulk metal to the adcluster considered by DAM is important, though this cannot be dealt with by the conventional cluster model.

Table 1 shows Mulliken's atomic charges of the  $AgO_2$  adcluster with  $R_{Ag-O} = 2.20$  Å and  $R_{O-O} = 1.35$  Å. In the  $^4\Sigma^+$  state, which does not involve electron transfer from the bulk metal, as mentioned above, the charge of  $O_2$  is small. The large negative charge  $-0.75$  of  $O_2$  in the  $^2\Pi$  state is transferred from the Ag atom alone, since no electron is supplied from the bulk metal. This electron transfer is unfavorable in energy as seen in Fig. 2. On the other hand, in

TABLE 1. Mulliken's atomic charges for the Ag— $O_a$ — $O_b$  adcluster<sup>a</sup>

State	$n$	Mulliken's atomic charge			
		Ag	$O_a$	$O_b$	$O_a + O_b$
$^4\Sigma^{+b}$	0.0	-0.103	-0.017	+0.120	+0.103
$^2\Pi^b$	0.0	+0.751	-0.637	-0.114	-0.751
$^3\Pi^b$	1.0	-0.328	-0.507	-0.165	-0.672
$^3A^{nc}$	1.0	-0.184	-0.501	-0.315	-0.816

<sup>a</sup>Ag—O and O—O lengths are at 2.20 and 1.35 Å, respectively.

<sup>b</sup>Linear Ag—O—O adcluster.

<sup>c</sup>Declining angle  $\theta$  of 70°.

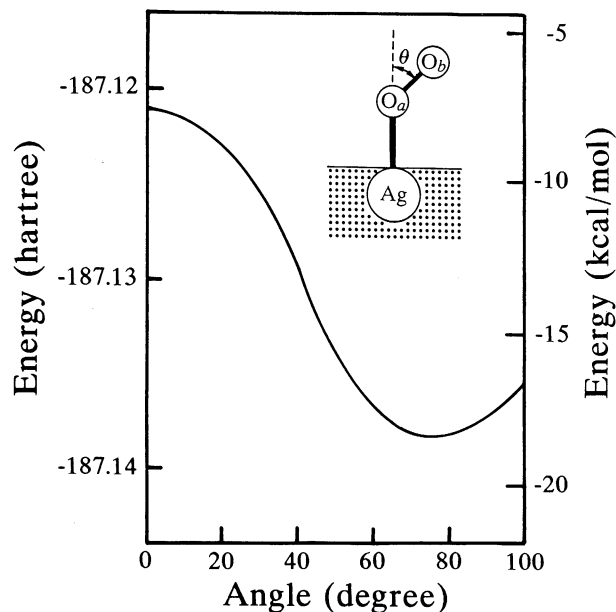


FIG. 3. Potential energy curve for the ground state of the  $AgO_2$  adcluster calculated by the SD-CI method for the  $O_2$  declining process. The declining angle  $\theta$  is defined in the figure. The Ag— $O_a$  and  $O_a$ — $O_b$  lengths are fixed at 2.20 and 1.35 Å, respectively. The energy scale on the right-hand side is in kcal/mol relative to the free Ag plus  $O_2$  system.

the  $^3\Pi$  state all the electrons transferred to  $O_2$  are supplied from the bulk metal. Note that the charge distribution of  $O_2$  in the  $^3\Pi$  state, the superoxide described by the DAM, is similar to that in the  $^2\Pi$  state, the superoxide in the cluster model. The negative charge on the Ag atom seems to reflect the smallness of the size of the adcluster. It also seems to be due to the use of the highest spin coupling model, which is an extreme model. Actually, in the calculation of the  $PdO_2$  adcluster based on the paired spin coupling model, the Pd atom has positive charge (9).

### $O_2$ declining process

We examine the O—O axis declining on the silver surface. While the  $\pi^*$  MOs of  $O_2$ , which have three electrons for the superoxide species, are degenerate in the linear system, they are separated into  $a'$  MO (in-plane) and  $a''$  MO (out-of-plane) in the declining process. The  $^3A''$  state, in

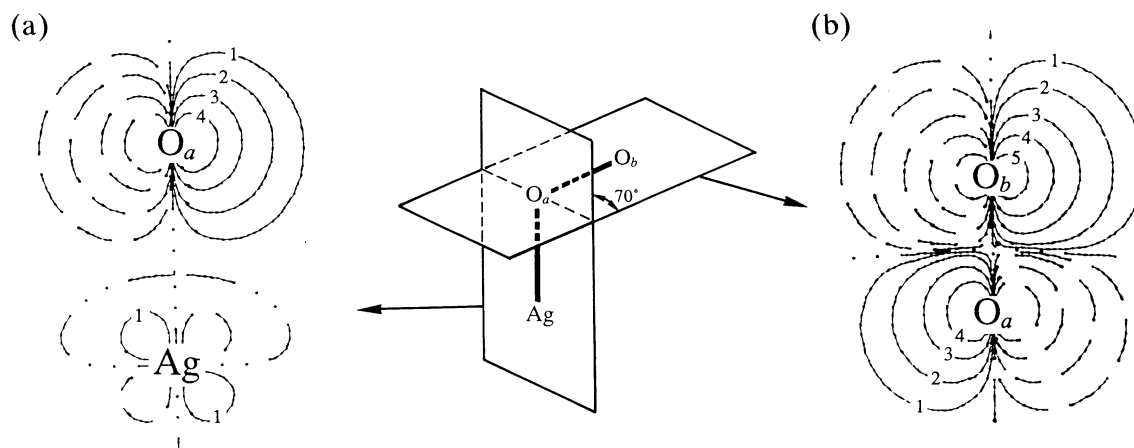


FIG. 4. Contour maps of the frontier orbital of the superoxide on silver calculated from the  $\text{AgO}_2$  adcluster with  $\text{Ag}-\text{O}_a$  and  $\text{O}_a-\text{O}_b$  distances of 2.20 and 1.35 Å, respectively, and the declining angle  $\theta$  of 70°; (a) and (b) are the maps on the planes including the  $\text{Ag}-\text{O}_a$  and  $\text{O}_a-\text{O}_b$  bonds, respectively. Solid and broken lines correspond to plus and minus signs in the MO. Double dotted line shows the node of the MO. The numbers 1–5 on the contours correspond to the values 0.01, 0.03, 0.10, 0.30, 1.00, respectively.

which the  $\pi^*$  MOs are splitting into doubly occupied  $a'$  and singly occupied  $a''$  MOs, is more stable than the  ${}^3A'$  state, in which the occupations in the  $\pi^*$  MOs are reversed. Figure 3 shows the potential energy curve of the  ${}^3A''$  state for the declining angle from the linear system. It is calculated by the SD-CI method with the  $\text{Ag}-\text{O}$  and  $\text{O}-\text{O}$  distances fixed at 2.20 and 1.35 Å, respectively. We find a minimum at the declining angle of 70–80°, which is similar to the result of Broomfield and Lambert (17). The energy at the minimum is more stable by 10.4 kcal/mol than that of the linear system. The adsorption energy is calculated to be 18.0 and 29.8 kcal/mol, relative to the energies of the separated system calculated for free molecules and supermolecule, respectively. The experimental value is 9.2 kcal/mol (25). The calculated state corresponds to the superoxide species, and no peroxide species is found in the lower energy region.

At the potential minimum, the net charges on  $\text{O}_a$  and  $\text{O}_b$  are calculated to be  $-0.50$  and  $-0.32$ , respectively, as shown in Table 1. Namely, the negative charge on the inside  $\text{O}_a$  atom is larger than that on the outside  $\text{O}_b$  atom, which seems to be opposite to the charge distribution expected from the covalent  $\text{Ag}-\text{O}-\text{O}^-$  system.

### Reactivity of superoxide

The frontier orbital of the superoxide species is the out-of-plane  $\pi^*$  MO, which is the singly occupied (SO) MO, while the in-plane  $\pi^*$  MO is doubly occupied as mentioned above. Figure 4 illustrates the frontier orbital map, which is related to the reactivity of the adsorbed oxygen species. Figures 4(a) and (b) correspond to the maps on the planes including the  $\text{Ag}-\text{O}_a$  and  $\text{O}_a-\text{O}_b$  bonds, respectively. These figures show much contribution of the  $\pi^*$  orbital of  $\text{O}_2$ , but little of the  $4d_{yz}$  orbital of Ag. Furthermore, in contrast to the charge distribution, the frontier orbital is larger at  $\text{O}_b$  than at  $\text{O}_a$ , which indicates that the former is more reactive than the latter.

Finally, we summarize the properties of the superoxide in the end-on form in contrast to the side-on dioxygen species studied in the previous work (7).

1. The  $\text{O}-\text{O}$  bond of the superoxide is moderately relaxed: Since the  $\pi^*$  orbitals of the species are formally oc-

cupied by three electrons, the  $\text{O}-\text{O}$  bond is weaker than the neutral species, but stronger than the peroxide species. As shown in the previous paper (7), the peroxide species leads to the dissociative oxygen on an Ag surface.

2. In the end-on geometry, the superoxide is not liable to become the peroxide: The present study shows that in the end-on geometry the superoxide is the ground state and no peroxide state exists in the lower energy region. On the contrary, the superoxide in the side-on form seems to be easily transformed into the peroxide, since the peroxide is more stable than the superoxide (7).

3. The outside oxygen of the superoxide is more reactive than the inside oxygen: The amplitude of the frontier orbital is larger at the outside oxygen than at the inside one, in contrast to the charge distribution. Furthermore, since the frontier orbital, which is SOMO, is mainly composed of the  $\pi^*$  MO of  $\text{O}_2$ , one-electron flow into this orbital causes a breaking of the  $\text{O}-\text{O}$  bond.

4. The charge distribution of the end-on superoxide is favorable for the approach of electron-rich molecules: By the above reasoning, the electron-rich molecule may attack the outside oxygen of the end-on superoxide. The electrostatic repulsion in this attacking process is reduced, since the negative charge on the outside oxygen atom is smaller than that on the inside one. On the other hand, in the side-on form there is no charge polarization between the two oxygen atoms.

### Acknowledgements

One of the authors (H. Nakatsuji) would like to thank Mr. N. Kishimoto of Nippon Shokubai Co., Ltd. for valuable discussions at the beginning of this study. The calculations were carried out with the FACOM M780 computer at the Data Processing Center of Kyoto University and the HITAC M-680H at the Institute for Molecular Science. The author thanks the IMS computer center for the grants of computing time. Part of this study was supported by the Grant-in-Aid for Scientific Research from the Japanese Ministry of Education, Science, and Culture, and by the Kurata Foundation.

1. A. Ayame and H. Kanoh. *Shokubai*, **20**, 381 (1978), in Japanese.
2. G. H. Twigg. *Proc. R. Soc. London, A*: **188**, 92 (1946).
3. E. L. Force and A. T. Bell, *J. Catal.* **40**, 356 (1975).
4. N. W. Cant and W. K. Hall. *J. Catal.* **52**, 81 (1978).
5. D. A. Outka, J. Stöhr, W. Jark, P. Stevens, J. Solomon, and R. J. Madix. *Phys. Rev. B*, **35**, 4119 (1987); J. Stöhr and D. A. Outka. *Phys. Rev. B*, **36**, 7891 (1987).
6. K. Bange, T. E. Madey, and J. K. Sass. *Chem. Phys. Lett.* **113**, 56 (1985).
7. H. Nakatsuji and H. Nakai. *Chem. Phys. Lett.* **174**, 283 (1990).
8. H. Nakatsuji. *J. Chem. Phys.* **87**, 4995 (1987).
9. H. Nakatsuji, H. Nakai, and Y. Fukunishi. *J. Chem. Phys.* **95**, 640 (1991).
10. H. Nakatsuji and K. Hirao. *J. Chem. Phys.* **68**, 2035 (1978); H. Nakatsuji. *Chem. Phys. Lett.* **59**, 362 (1978); **67**, 329 (1979); **67**, 334 (1979).
11. H. Nakatsuji. *Reports in molecular theory*. CRC Press, Boca Raton, FL. In press.
12. A. Selmani, J. M. Sichel, and D. R. Salahub. *Surf. Sci.* **157**, 208 (1985); A. Selmani, J. Andzelm, and D. R. Salahub. *Int. J. Quantum Chem.* **29**, 829 (1986).
13. M. L. McKee. *J. Chem. Phys.* **87**, 3143 (1987).
14. T. H. Upton, P. Stevens, and R. J. Madix. *J. Chem. Phys.* **88**, 3988 (1988).
15. E. A. Carter and W. A. Goddard III. *Surf. Sci.* **209**, 243 (1989).
16. P. J. van den Hoek and E. J. Baerends. *Surf. Sci.* **221**, L791 (1989); P. J. van den Hoek, E. J. Baerends, and R. A. van Santen. *J. Phys. Chem.* **93**, 646 (1989).
17. K. Broomfield and R. M. Lambert, *Mol. Phys.* **66**, 421 (1989).
18. P. J. Hay and W. R. Wadt. *J. Chem. Phys.* **82**, 270 (1985).
19. S. Huzinaga. *J. Chem. Phys.* **42**, 1293 (1965); T. H. Dunning, Jr. *J. Chem. Phys.* **53**, 2823 (1970).
20. T. H. Dunning, Jr. and P. J. Hay. *In Modern theoretical chemistry*. Vol. 3. Edited by H. F. Schaeffer III. Plenum, New York. 1977.
21. E. Sutton. *Tables of interatomic distances and configuration in molecules and ions*. The Chemical Society, London. 1965.
22. K. P. Huber and G. Herzberg. *Molecular spectra and molecular structure*. IV. Constants of diatomic molecules. Van Nostrand Reinhold, New York. 1979.
23. A. W. Dweydari and C. H. B. Mee. *Phys. Status Solidi A*: **27**, 223 (1975).
24. B. R. Brooks, P. Saxe, W. D. Laidig, and M. Dupuis. Program System GAMESS; Program Library No. 481, Computer Center of the Institute for Molecular Science, Okazaki. 1981.
25. C. T. Campbell. *Surf. Sci.* **157**, 43 (1985).